The University of Manchester
Wolfson Molecular Imaging Centre

MANCHESTER 1824

PET data analysis - human studies with [^{11}C](*R*)-PK11195 and beyond

Rainer Hinz

07th October 2014

Århus PET-Center

MANCHESTER 1824

Contents

- Introduction
- Overview of [^{11}C](*R*)- PK11195 as an imaging marker
- Plasma input function modelling
- Reference tissue input function modelling
- Reference tissue input function extraction
- Ongoing clinical research studies in psoriasis, depression and schizophrenia
- Developments in pre-clinical data analysis
- Outlook
- Acknowledgements

MANCHESTER 1824

Introduction

Translocator Protein 18kDa (TSPO)

- is a nuclear encoded mitochondrial protein.
- is abundant in peripheral organs (particularly adrenal glands and kidney) and haematogenous cells.
- its function still needs full elucidation but it plays an important role in steroid synthesis and in the regulation of immunological responses in mononuclear phagocytes.

TSPO in diseases of the Central Nervous System (CNS)

- High levels have been observed in infiltrating blood-borne cells and activated microglia.
- Significant microglial activation occurs after mild to severe neuronal damage resulting from traumatic, inflammatory, degenerative and neoplastic disease.
- Microglia are activated in the surroundings of focal lesions but also in the distant, anterograde and retrograde projection areas of the lesioned neural pathway.

[^{11}C](*R*)- PK11195 as an imaging marker

- PK11195 is a selective ligand for TSPO and the reference compound for TSPO binding assays

PubMed.gov
US National Library of Medicine
National Institutes of Health

PubMed | PK11195 | Search
RSS | Save search | Advanced | Help

Show additional filters

Article types
Clinical Trial
Review
More ...

Text availability
Abstract
Free full text
Full text

Publication dates
5 years
10 years
Custom range...

Species
Humans
Other Animals

Clear all

Show additional filters

Display Settings: Summary, 20 per page, Sorted by Recently Added | Send to:

Results: 1 to 20 of 1248

<< First | < Prev | Page 1 of 63 | Next > | Last >>

1. Influence of microglial activation on neuronal function in Alzheimer's and Parkinson's disease dementia.
Fan Z, Aman Y, Ahmed I, Chetelat G, Brigitte L, Ray Chaudhuri K, Brooks DJ, Edison P.
Alzheimers Dement. 2014 Sep 16. pii: S1552-5260(14)02501-1. doi: 10.1016/j.jalz.2014.06.016. [Epub ahead of print]
PMID: 25239737 [PubMed - as supplied by publisher]
Related citations

2. Comparison of in vivo binding properties of the 18-kDa translocator protein (TSPO) ligands [^{18}F]PBR102 and [^{18}F]PBR111 in a model of excitotoxin-induced neuroinflammation.
Callaghan PD, Wimberley CA, Rahardjo GL, Berghofer PJ, Pham TQ, Jackson T, Zahra D, Bourdier T, Wyatt N, Greguric I, Howell NR, Siegele R, Pastuovic Z, Mattner F, Loc'h C, Gregoire MC, Katsifis A.
Eur J Nucl Med Mol Imaging. 2014 Sep 18. [Epub ahead of print]
PMID: 25231248 [PubMed - as supplied by publisher]
Related citations

3. Non-invasive imaging of vascular inflammation.
Ammirati E, Moroni F, Pedrotti P, Scotti I, Magnoni M, Bozzolo EP, Rimoldi OE, Camici PG.
Front Immunol. 2014 Aug 18;5:399. doi: 10.3389/fimmu.2014.00399. eCollection 2014. Review.
PMID: 25183963 [PubMed] Free PMC Article

Filters: Manage Filters

New feature
Try the new Display Settings option - **Sort by Relevance**

Results by year

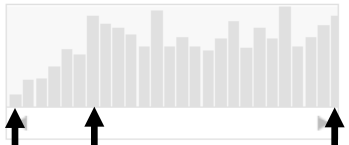

Download CSV

PMC Images search for *PK11195*

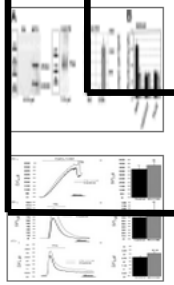

2014: 49
(23 Sep 2014)

1989: 52

1983: 7

[^{11}C](*R*)- PK11195 as an imaging marker

Peripheral-type benzodiazepine receptors in the living heart characterized by positron emission tomography *Circulation 73, No. 3, 476–483, 1986.*

PIERRE CHARBONNEAU, M.D., ANDRÉ SYROTA, M.D., PH.D., CHRISTIAN CROUZEL, PH.D., JEAN-MARIE VALOIS, B.S., CHRISTIAN PRENANT, B.S., AND MONIQUE CROUZEL

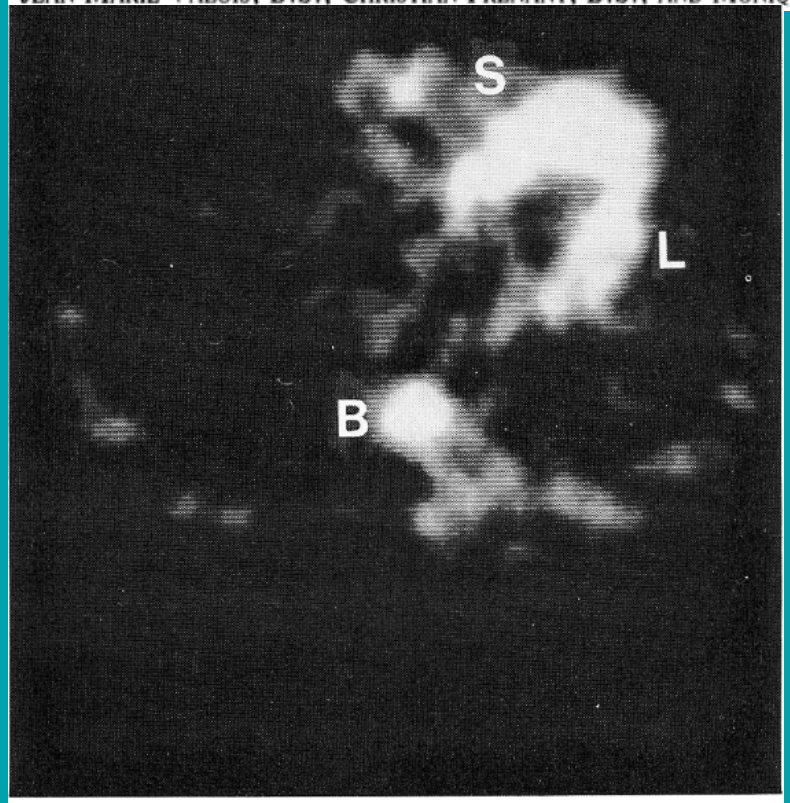

FIGURE 5. PET image of a human heart after intravenous injection of ^{11}C–PK 11195. The PET scan was obtained 15 min after injection of ^{11}C–PK 11195 (12.3 mCi, specific activity 484 mCi/μmol). At this time the septum (S) and of the lateral wall of the left ventricle (L) were clearly visualized. Radioactivity in the lung was low. B = bone marrow.

The injection of various amounts of PK 11195 (100, 200, or 500 µg/kg body weight) 30 min after injection of the labeled ligand led to a rapid fall in radioactivity in the heart.

TABLE 2
Myocardial uptake and binding inhibition of bound ^{11}C–PK 11195 by excess unlabeled PK 11195 in four human volunteers

	Amount of ^{11}C–11195 injected (nmol/kg)	Myocardial uptake (% × 10^{-3})	Amount of unlabeled PK 11195 (μg/kg)	^{11}C–PK 11195 binding inhibition (%)
PKH 004	2.47	10	100	25
PKH 002	0.40	8	200	34
PKH 003	0.90	8	200	34
PKH 006	0.94	7.5	500	48

A linear correlation was demonstrated between the concentration of PK11195 in the heart (expressed as pmol/cm^3) and the amount of PK 11195 injected for doses below 3 nmol/kg (r = .991).

[^{11}C](*R*)- PK11195 as an imaging marker

Junck L, Olson JMM, Ciliax BJ, Koeppe RA, Watkins GL, Jewett DM, McKeever PE, Wieland DM, Kilbourn MR, Starosta-Rubinstein S, Mancini WR, Kuhl DE, Greenberg HS, Young AB. PET imaging of human gliomas with ligands for the peripheral benzodiazepine binding site. Ann Neurol 1989;26:752–758

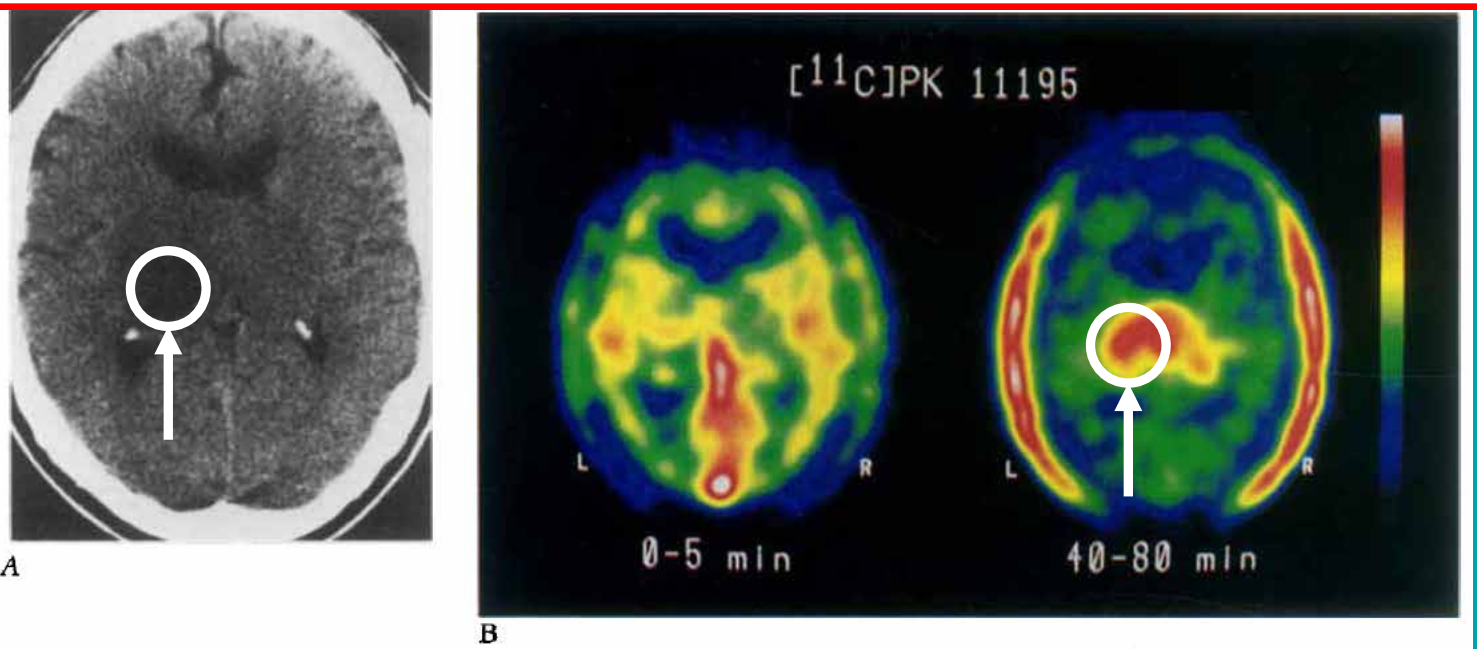

Fig 3. Patient with astrocytoma of indeterminate grade, as proved by examination of biopsy specimen. (A) Computed tomographic scan after infusion of contrast medium. The tumor in the left thalamus does not manifest contrast enhancement. A slight decrease in attenuation extends into the right thalamus. (B) Positron emission tomographic scans performed 0 to 5 and 40 to 80 minutes after injection of {^{11}C}PK 11195. Radioactivity in the later images is highest in tumor (1.88 times that in remote gray matter) and in scalp. Increased radioactivity extends into the right thalamus.

Table 4. Transfer Constant (K_1), Blood Flow, and Unidirectional Extraction from {^{11}C}PK 11195 Positron Emission Tomographic Studies (n = 4)[a]

	K_1 (ml/gm · min)	Blood Flow (ml/gm · min)	Extraction (%)
Tumor	0.027 ± 0.014	0.40 ± 0.17	7.5 ± 4.4
Gray matter	0.028 ± 0.011	0.55 ± 0.06	4.9 ± 1.4
White matter	0.013 ± 0.007	0.28 ± 0.08	4.4 ± 1.7

[a]Values represent mean ± SD.

[^{11}C](*R*)- PK11195 as an imaging marker

MANCHESTER 1824

Monitoring by PET of macrophage accumulation in brain after ischaemic stroke

S. C. Ramsay
C. Weiller
R. Myers
J. E. Cremer
S. K. Luthra
A. A. Lammertsma
R. S. J. Frackowiak

THE LANCET
VOL 339: APRIL 25, 1992

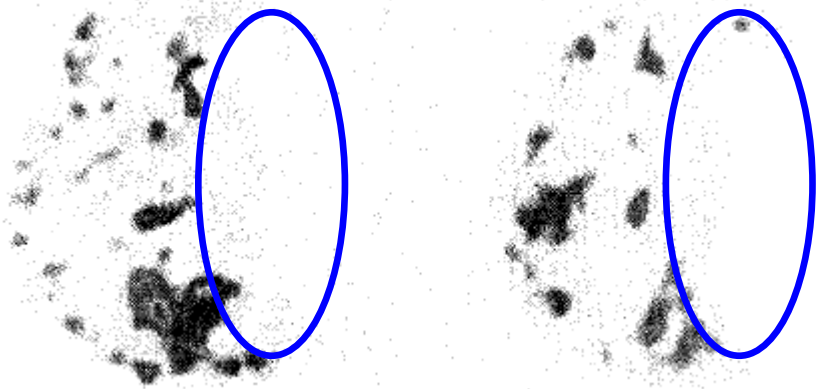

Fig 1—Sample transaxial slices of CBF scan.

Large area of hypoperfusion in left hemisphere, as indicated by blue area on right

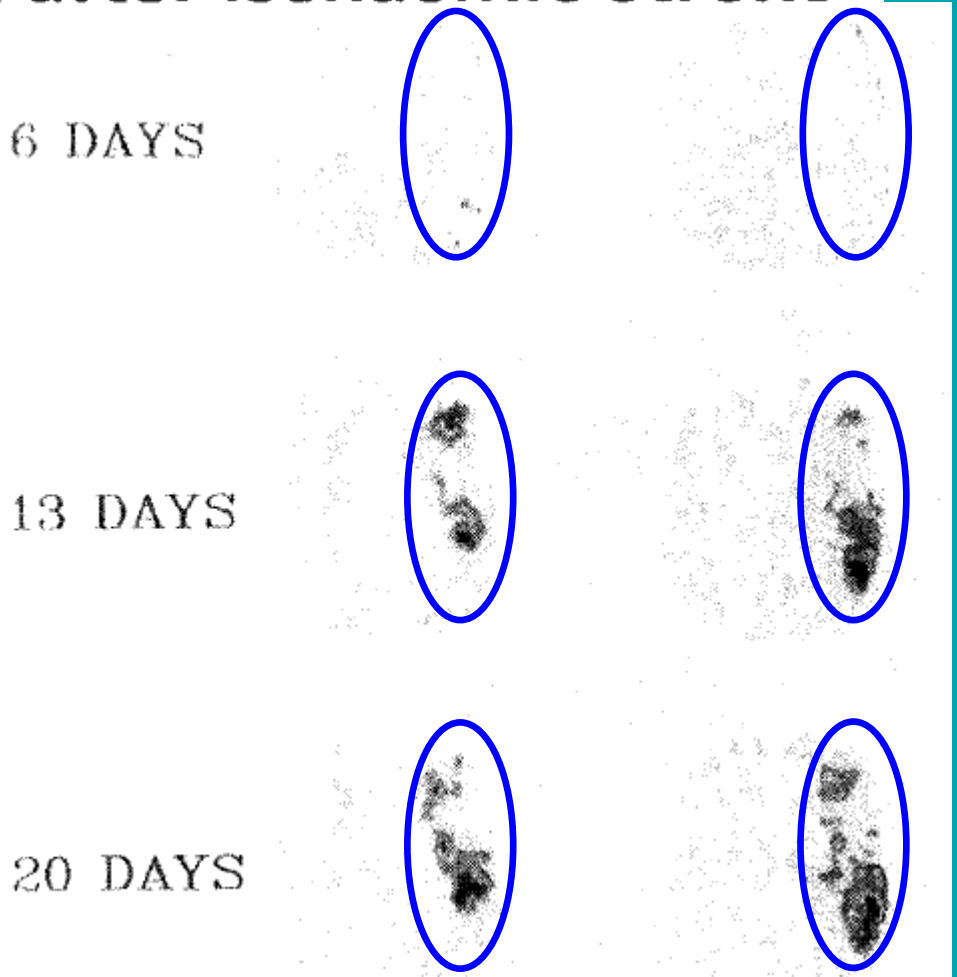

Fig 2—Sample transaxial [^{11}C]-PK 11195 images showing comparable slices for the 3 days.

[^{11}C](*R*)- PK11195 as an imaging marker

MANCHESTER 1824

In-vivo measurement of activated microglia in dementia

Annachiara Cagnin, David J Brooks, Angus M Kennedy, Roger N Gunn, R Myers, Federico E Turkheimer, Terry Jones, Richard B Banati

THE LANCET • Vol 358 • August 11, 2001

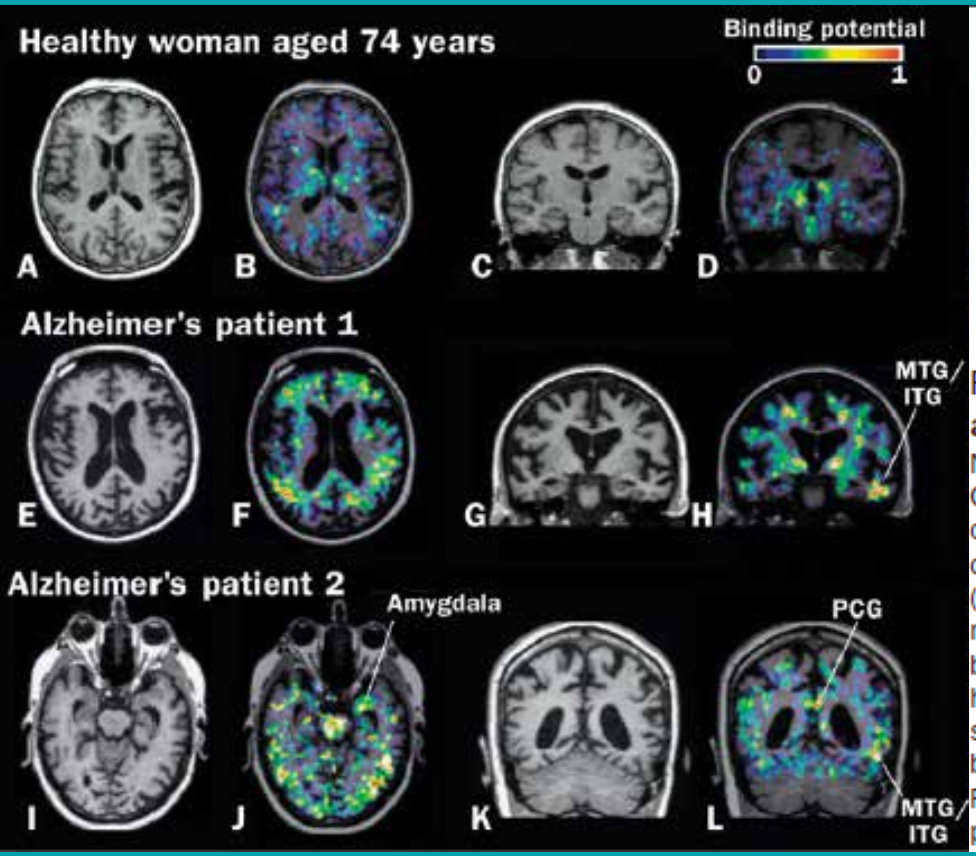

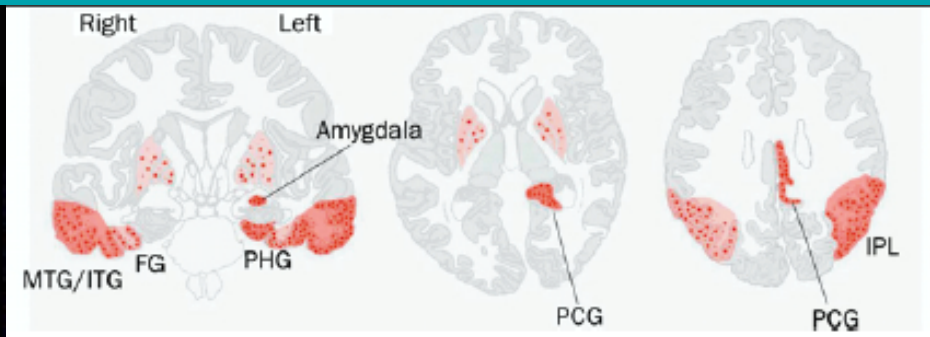

Figure 2: **[^{11}C]*(R)*-PK11195 binding in healthy elderly controls and patients with Alzheimer's disease**

No significant [^{11}C]*(R)*-PK11195 binding is seen in healthy cortex (A, C [T1-weighted MRI], B, D [MRI-PET fusion image]); however, widespread cortical [^{11}C]*(R)*-PK11195 binding is seen in the patient with severe dementia (E–H), with a prominent signal in the left temporal lobe (MTG/ITG=middle and inferior temporal gyrus). In the patient with moderate dementia (I–L), substantial [^{11}C]*(R)*-PK11195 binding is seen bilaterally in the temporal lobe but more pronounced in the left hemisphere (PCG=posterior cingulate gyrus). Schematic drawing summarises anatomical distribution pattern of peripheral benzodiazepine binding sites (red areas) in Alzheimer's disease (FG=fusiform gyrus, PHG=parahippocampal gyrus, PCG=posterior cingulate gyrus, IPL=inferior parietal lobe).

The University of Manchester
Wolfson Molecular Imaging Centre

Plasma input function modelling

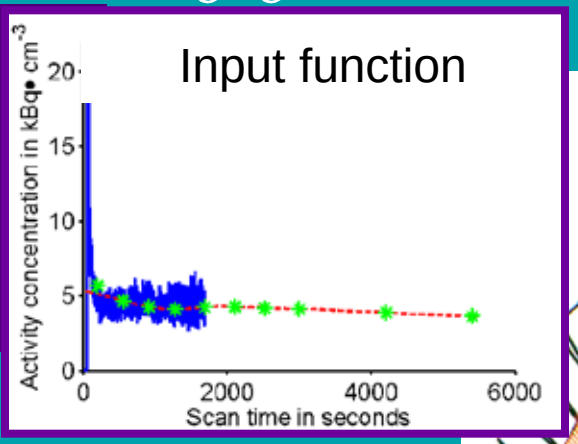

Peripheral detector systems
(bioanalysis)

tubing

Radial artery

Lungs

Kinetic modelling

plasma $c_p(t)$

K_1

k_2

$c_1(t)$

tissue $c_t(t)$

PET scanner

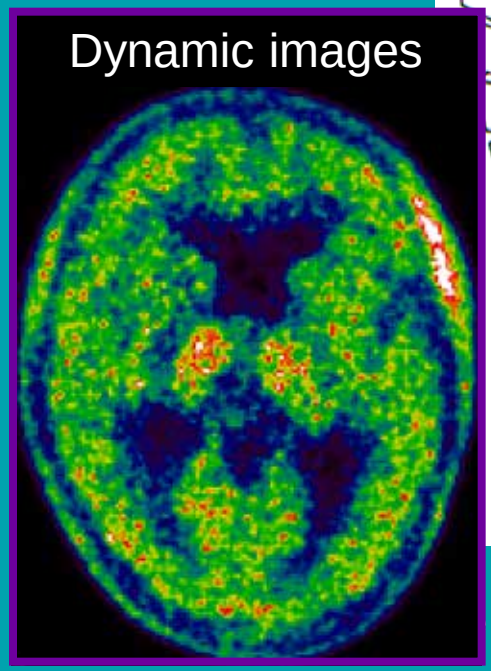

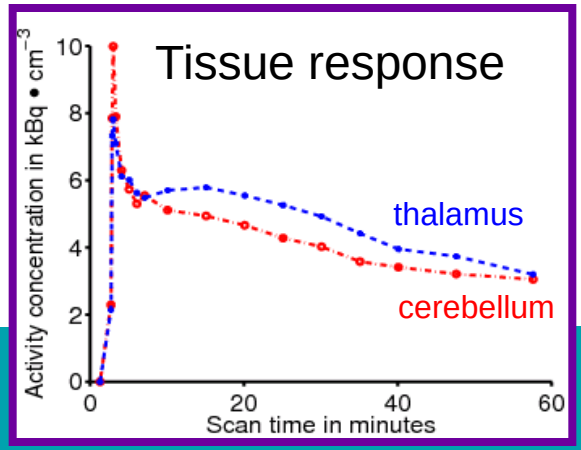

The University of Manchester
Wolfson Molecular Imaging Centre

Plasma input function modelling

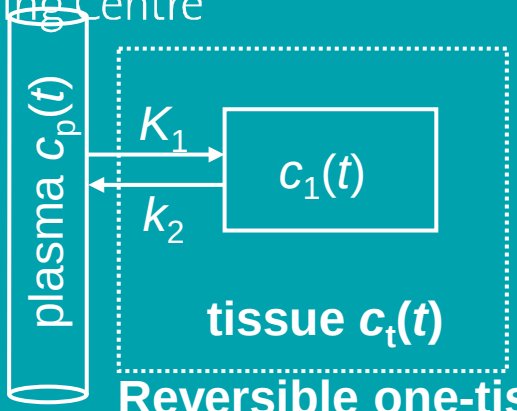

Reversible one-tissue compartment model (1TCM)

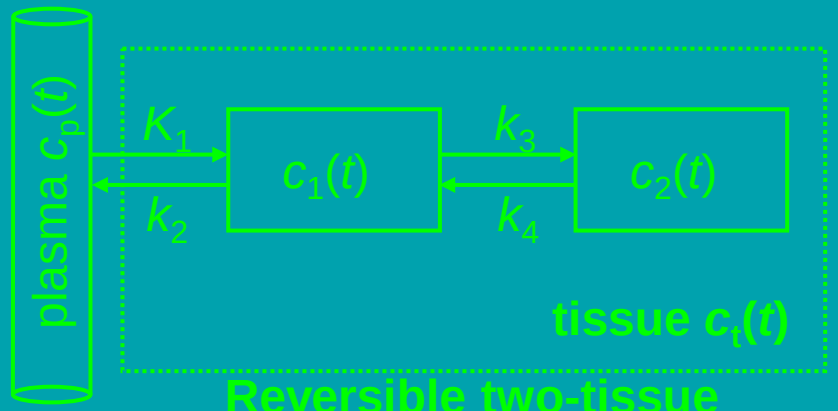

Reversible two-tissue compartment model (2TCM)

Development of a tracer kinetic plasma input model for *(R)*-[^{11}C]PK11195 brain studies

Journal of Cerebral Blood Flow & Metabolism (2005) 25, 842–851

Marc A Kropholler[1], Ronald Boellaard[1], Alie Schuitemaker[1,2], Bart NM van Berckel[1,*], Gert Luurtsema[1], Albert D Windhorst[1] and Adriaan A Lammertsma[1]

It was concluded that a two-tissue reversible compartment model with K_1/k_2 fixed to whole cortex value is optimal for analyzing *(R)*-[^{11}C]PK11195 PET brain studies.

Kinetic analysis and test-retest variability of the radioligand [^{11}C](R)-PK11195 binding to TSPO in the human brain - a PET study in control subjects

Aurelija Jučaite[1*], Zsolt Cselényi[1], Annie Arvidsson[1], Gabrielle Åhlberg[1], Per Julin[1], Katarina Varnäs[2], Per Stenkrona[2], Jan Andersson[2], Christer Halldin[2] and Lars Farde[1,3]

EJNMMI Research 2012, **2**:15

[^{11}C](*R*)-PK11195 binding could be described by 2TCM which was the preferred model.

Plasma input function modelling

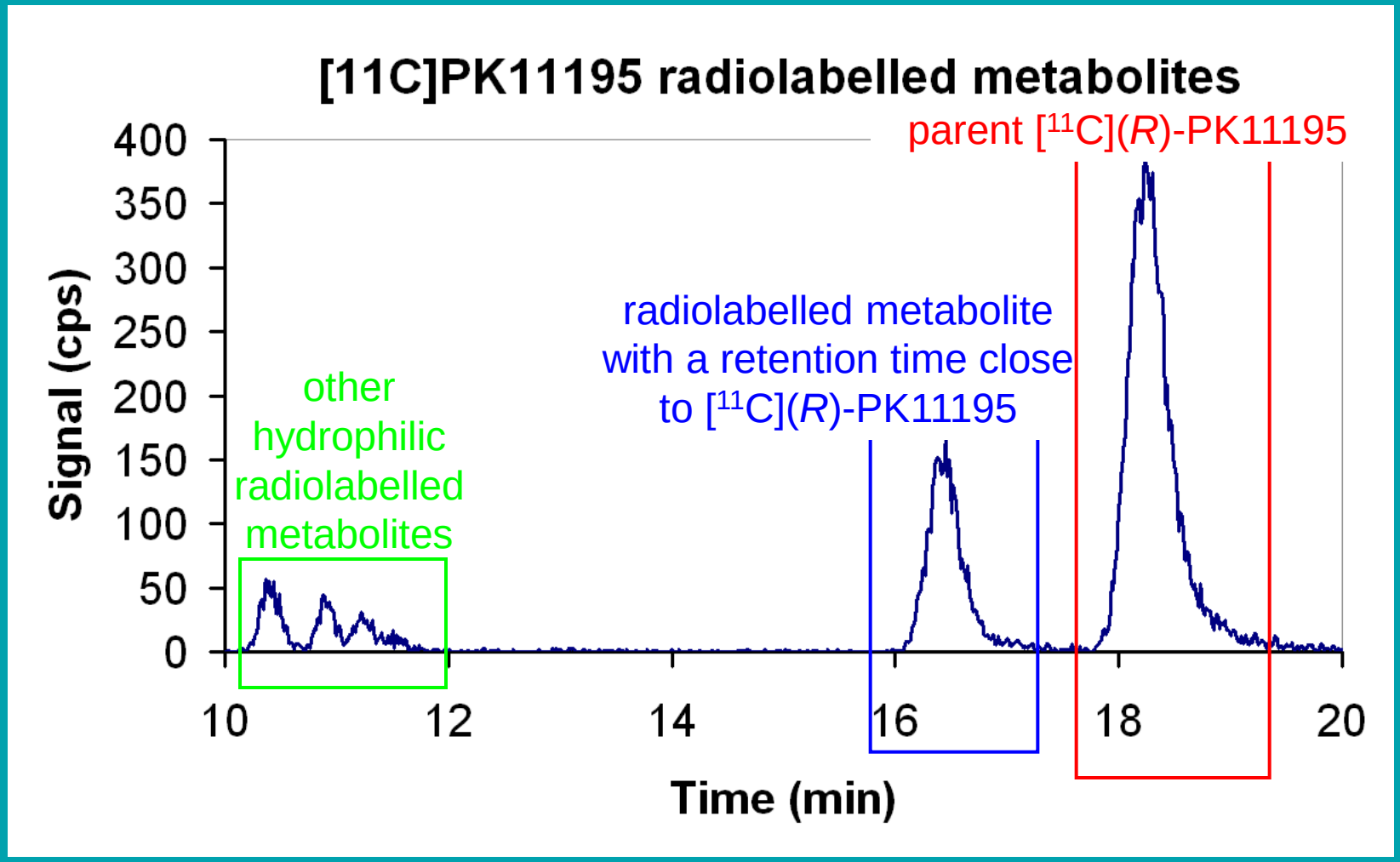

Example radiochromatogram obtained from an essay with hepathic microsomes.

Plasma input function modelling

Detection and Quantification of Large-Vessel Inflammation with ^{11}C-(*R*)-PK11195 PET/CT

J Nucl Med 2011; 52:33–39

Frederic Lamare[1], Rainer Hinz[2], Oliver Gaemperli[1], Francesca Pugliese[1], Justin C. Mason[3], Terence Spinks[4], Paolo G. Camici[1,5], and Ornella E. Rimoldi[1,6]

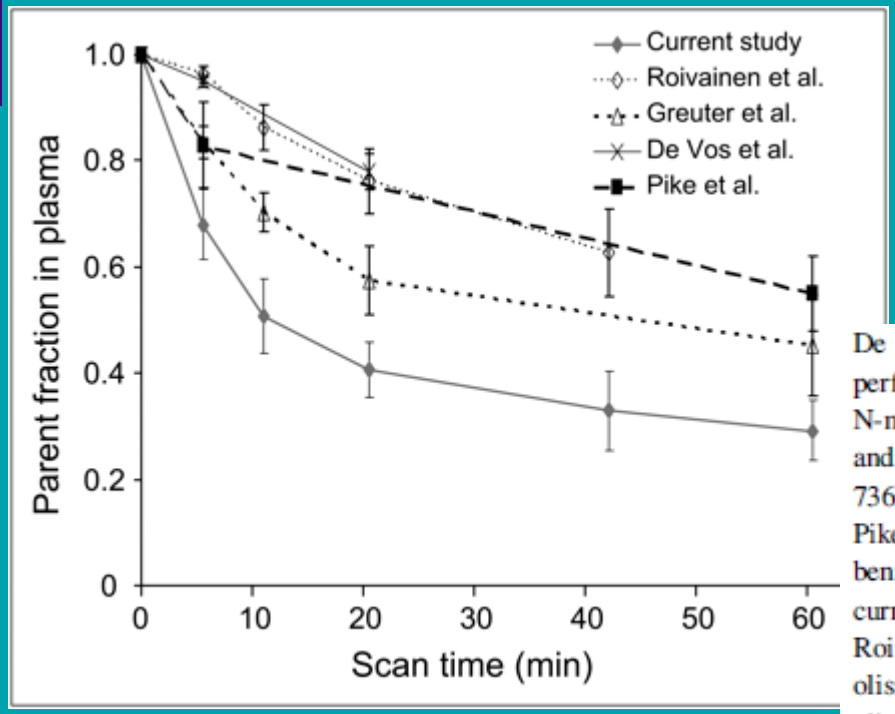

De Vos F, Dumont F, Santens P, Slegers G, Dierckx R, De Reuck J. High-performance liquid chromatographic determination of [^{11}C]-1-(2-chlorophenyl)-N-methyl-N-(1-methylpropyl)-3-isoquinoline carboxamide in mouse plasma and tissue and in human plasma. *J Chromatogr B Biomed Sci Appl.* 1999; 736:61–66.

Pike VW, Halldin C, Crouzel C, et al. Radioligands for PET studies of central benzodiazepine receptors and PK (peripheral benzodiazepine) binding sites: current status. *Nucl Med Biol.* 1993;20:503–525.

Roivainen A, Nagren K, Hirvonen J, et al. Whole-body distribution and metabolism of [N-methyl-^{11}C](R)-1-(2-chlorophenyl)-N-(1-methylpropyl)-3-isoquinolinecarboxamide in humans: an imaging agent for in vivo assessment of peripheral benzodiazepine receptor activity with positron emission tomography. *Eur J Nucl Med Mol Imaging.* 2009;36:671–682.

Greuter HNJM, van Ophemert PLB, Luurtsema G, et al. Optimizing an online SPE-HPLC method for analysis of (R)-[^{11}C]1-(2-chlorophenyl)-N-methyl-N-(1-methylpropyl)-3-isoquinolinecarboxamide [(R)-[^{11}C]PK11195] and its metabolites in humans. *Nucl Med Biol.* 2005;32:307–312.

Reference tissue input function modelling

Evaluation of reference tissue models for the analysis of [^{11}C](*R*)-PK11195 studies

Marc A Kropholler[1], Ronald Boellaard[1], Alie Schuitemaker[1,2], Hedy Folkersma[3], Bart NM van Berckel[1] and Adriaan A Lammertsma[1]

Journal of Cerebral Blood Flow & Metabolism (2006) 26, 1431–1441

Simplified reference tissue model is the best alternative when no plasma input is available.

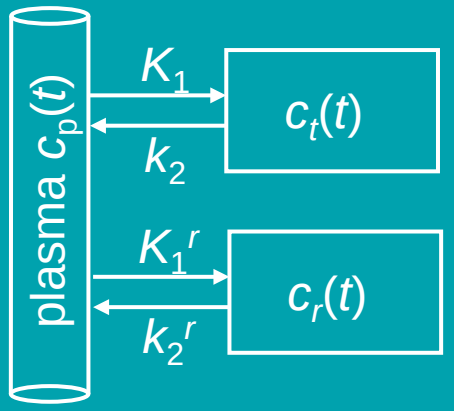

Simplified reference tissue model (SRTM)

Labelling of Peripheral-Type Benzodiazepine Binding Sites in Human Brain With [^{3}H]PK 11195: Anatomical and Subcellular Distribution

A. DOBLE, C. MALGOURIS, M. DANIEL, N. DANIEL, F. IMBAULT, A. BASBAUM,* A. UZAN, C. GUÉRÉMY AND G. LE FUR

Brain Research Bulletin, Vol. 18, pp. 49–61, 1987.

Abbreviations	Structures		Binding Densities (fmol/mg protein)
Cerebellum			
CB	Cerebellar cortex	Granular cell layer	660 ± 85
		Molecular cell layer	191 ± 55
		White matter	41 ± 32
CBL, CBM, CBE	Deep cerebellar nuclei	Dentate nucleus	344 ± 74
		Fastigial nucleus	147 ± 43
		Interpositus nucleus	104 ± 62

The University of Manchester
Wolfson Molecular Imaging Centre

Reference tissue input function extraction

Adaptation of the mixture model algorithm by Hartigan (1975).

A Cluster Analysis Approach for the Characterization of Dynamic PET Data

JOHN ASHBURNER,[1] JANE HASLAM,[2] CHRIS TAYLOR,[2] VINCENT J. CUNNINGHAM,[1] and TERRY JONES[1]

[1]*Cyclotron Unit, Hammersmith Hospital, London W12 0NN, United Kingdom*
[2]*Medical Biophysics, Medical School, Manchester, United Kingdom*

QUANTIFICATION OF BRAIN FUNCTION USING PET

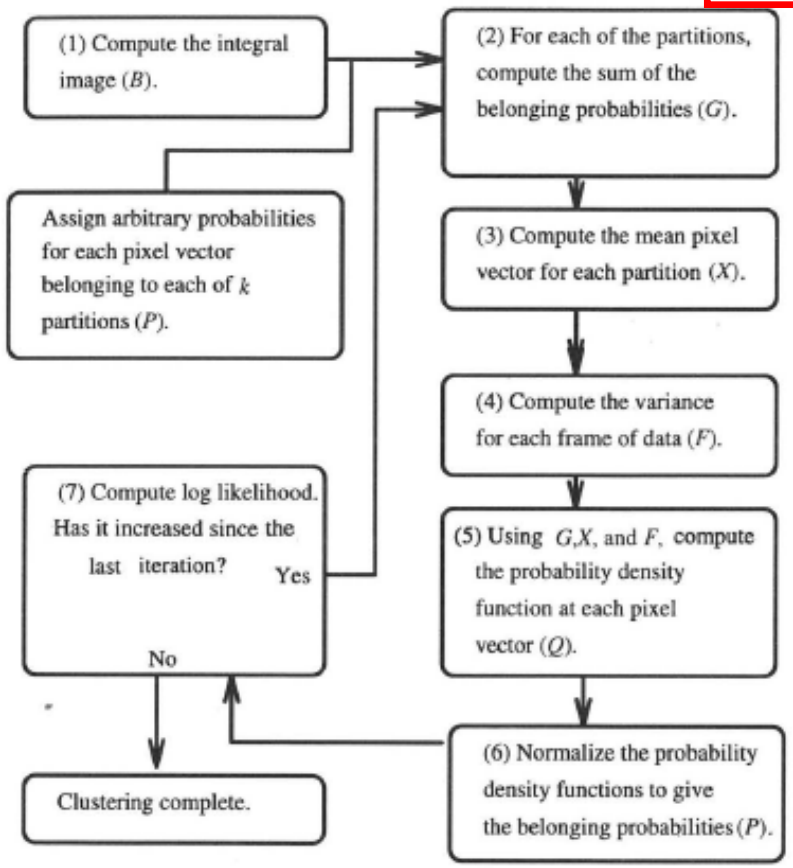

FIGURE 1 Flow diagram for clustering.

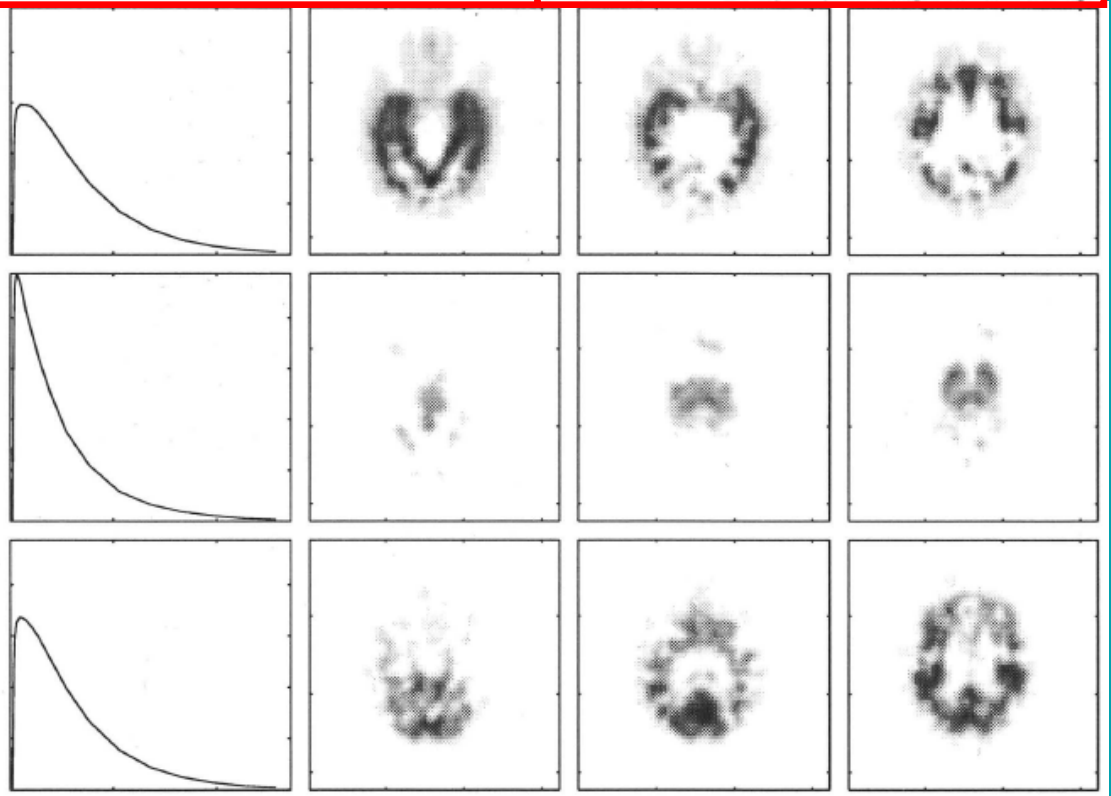

FIGURE 2 Cluster analysis applied to a dynamic flumazenil image. The three rows represent the clusters, and the columns are selected planes from the volume. The images are the likelihoods of belonging to each of the clusters, multiplied by the integral image. They have been smoothed slightly to improve visualization. The plot on the left is the cluster mean.

Reference tissue input function extraction

Brain (2000), **123**, 2321–2337

The peripheral benzodiazepine binding site in the brain in multiple sclerosis

Quantitative *in vivo* imaging of microglia as a measure of disease activity

R. B. Banati,[1,10] J. Newcombe,[4] R. N. Gunn,[1] A. Cagnin,[1] F. Turkheimer,[1] F. Heppner,[3,11] G. Price,[7] F. Wegner,[9] G. Giovannoni,[5] D. H. Miller,[5] G. D. Perkin,[3] T. Smith,[4,6] A. K. Hewson,[4,8] G. Bydder,[2] G. W. Kreutzberg,[10] T. Jones,[1] M. L. Cuzner[4] and R. Myers[1]

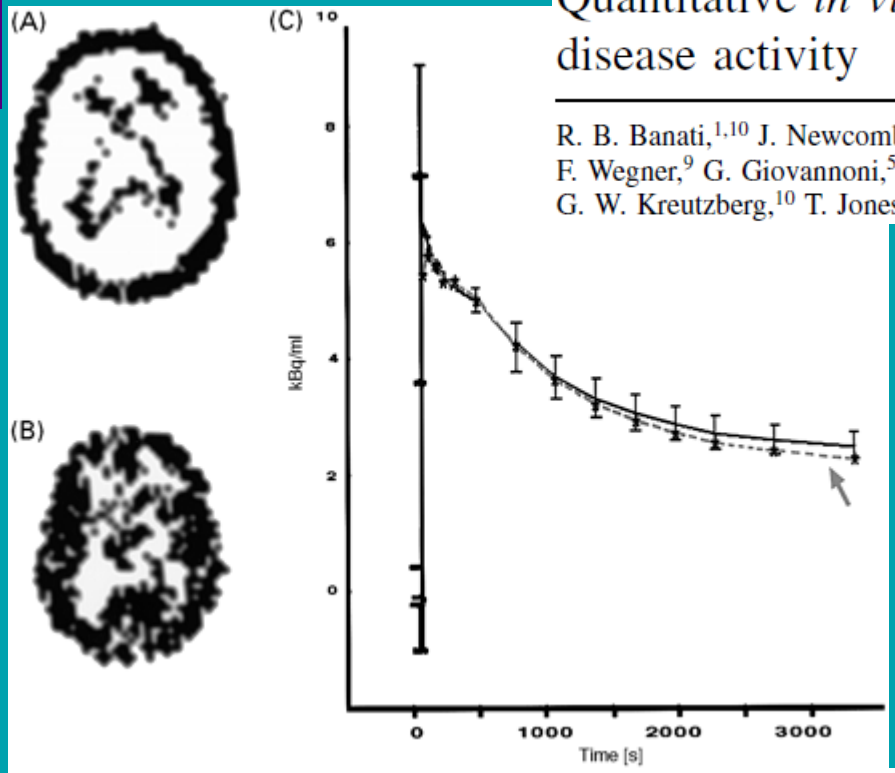

Limitation of the study and outlook

Binding of [^{11}C](*R*)-PK11195 was measured with a simplified reference region approach and cluster analysis that permitted the robust extraction of a normal reference kinetic without prior anatomical definition of a normal reference region. However, one patient with SP multiple sclerosis had to be excluded from this study since no appropriate concentration time–activity curve could be extracted to serve as an input function. This may indicate

Fig. 1 The majority of the time–activity curves extracted by cluster analysis from the dynamic [^{11}C](*R*)-PK11195 PET data of a normal brain fell into two clusters, one localizing to extracerebal structures (**A**) and the other to healthy brain tissue (**B**). The latter represents the normal reference kinetic that would have been obtained from an anatomically defined mask similar to that seen in **B**. The population input kinetic (solid line, with standard deviations) was used to decide whether an individual dynamic data set (here from Patient 9) contained a time–activity curve suitable to serve as the individual's reference input function (dotted line and arrow).

The University of Manchester
Wolfson Molecular Imaging Centre

MANCHESTER 1824

Reference tissue input function extraction

Reference and Target Region Modeling of [^{11}C]-(*R*)-PK11195 Brain Studies

J Nucl Med 2007; 48:158–167

Federico E. Turkheimer[1–3], Paul Edison[1,3], Nicola Pavese[3], Federico Roncaroli[4], Alexander N. Anderson[1], Alexander Hammers[1,5], Alexander Gerhard[3,6], Rainer Hinz[2], Yan F. Tai[1,3], and David J. Brooks[1–3]

Normalise each frame of the dynamic image by subtracting its mean and dividing it by its standard deviation to create a unit input.

Database of six kinetic classes extracted from reference scans
1. Normal grey matter
2. White matter
3. Blood pool
4. Muscle
5. Scull / bone
6. High density TSPO binding

Describe every pixel $P_i(t)$ as a weighted linear combination of the kinetic classes as:

$$P_i^n(t) = \sum_{j=1}^{6} w_{ij} K_j^n(t),$$

with $w_{ij} \geq 0$

$P_i^n(t)$ … normalised kinetic at voxel i

$K_j^n(t)$ … normalised kinetic class j (j= 1, …, 6)

Non-negative least squares (NNLS) algorithm to determine the set of weights w_{ij} per pixel.

Use the map w_{i1} of the normal grey matter kinetics to calculate the reference tissue kinetics.

Supervised Cluster Analysis with 6 classes (SVCA6)

Reference tissue input function extraction

Evaluation of reference regions for *(R)*-[^{11}C]PK11195 studies in Alzheimer's disease and Mild Cognitive Impairment

Marc A Kropholler[1], Ronald Boellaard[1], Bart NM van Berckel[1], Alie Schuitemaker[2], Reina W Kloet[1], Mark J Lubberink[1], Cees Jonker[3], Philip Scheltens[4] and Adriaan A Lammertsma[1]

Journal of Cerebral Blood Flow & Metabolism (2007) 27, 1965–1974

Gray matter, white matter, total cerebellum and cerebrum, and cluster analysis were evaluated as reference regions. […] For cerebellum white matter, cerebrum white matter, and total cerebrum a considerable number of unrealistic BP^{SRTM} values were observed. Cluster analysis did not extract a valid reference region in 10% of the scans. […] Most anatomic regions outperformed cluster analysis in terms of absence of both scan rejection and bias. **Total cerebellum is the optimal reference region in this patient category.**

Reference tissue input function extraction

[^{11}C]-(*R*)PK11195 tracer kinetics in the brain of glioma patients and a comparison of two referencing approaches

Zhangjie Su · Karl Herholz · Alexander Gerhard · Federico Roncaroli · Daniel Du Plessis · Alan Jackson · Federico Turkheimer · Rainer Hinz

Eur J Nucl Med Mol Imaging (2013) 40:1406–1419

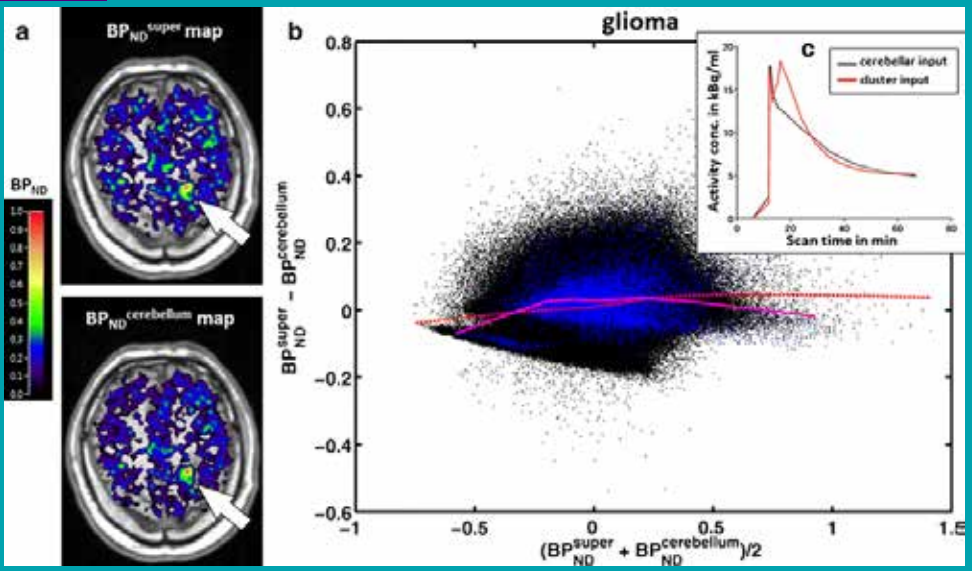

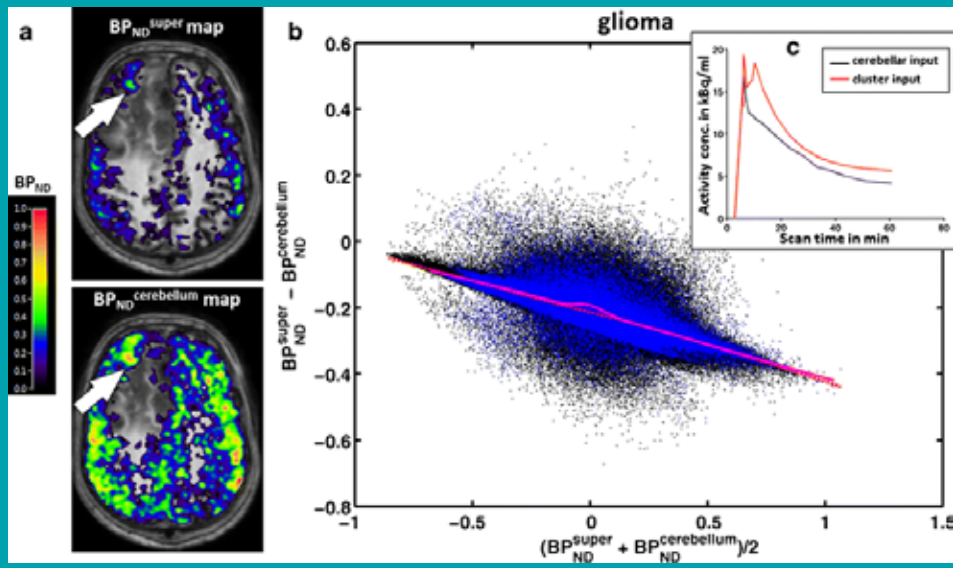

Supervised cluster and cerebellar input functions produced consistent BP_{ND} estimates in approximately half of the gliomas investigated, but had a systematic difference in the remainder. **The cerebellar input is preferred based on theoretical and practical considerations.**

The University of Manchester
Wolfson Molecular Imaging Centre

MANCHESTER 1824

Reference tissue input function extraction

Apply a brain mask to the dynamic data before normalisation.

Optimization of supervised cluster analysis for extracting reference tissue input curves in (*R*)-[^{11}C]PK11195 brain PET studies

Maqsood Yaqub[1], Bart NM van Berckel[1], Alie Schuitemaker[2], Rainer Hinz[3], Federico E Turkheimer[4], Giampaolo Tomasi[5], Adriaan A Lammertsma[1] and Ronald Boellaard[1]

Journal of Cerebral Blood Flow & Metabolism (2012) 32, 1600–1608

Only four kinetic classes:
1. Normal grey matter
2. White matter
3. Blood pool
4. High density TSPO binding

Supervised Cluster Analysis with Brain Mask (SVCA4)

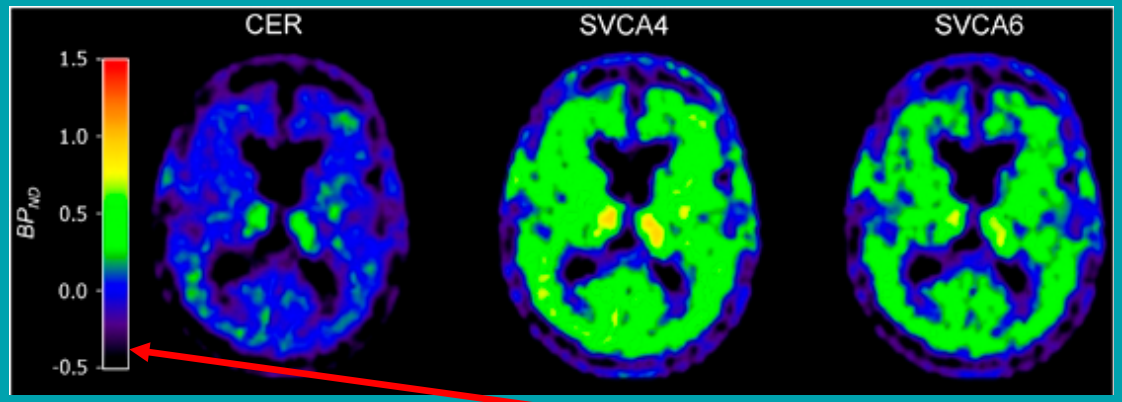

Figure 5 Parametric binding potential (BP_{ND}) images generated using reference tissue model Reference tissue inputs were taken from cerebellum (CER), SVCA4, and SVCA6. Data were taken from an AD subject.

Negative BP_{ND}

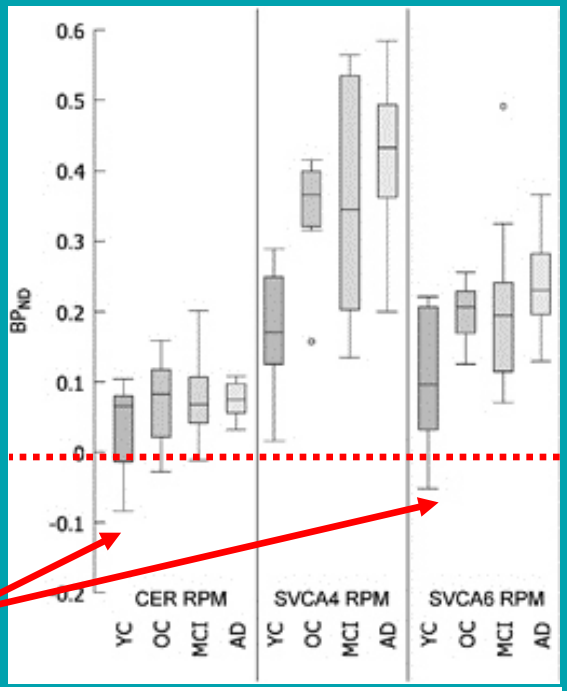

Figure 6 Comparison of thalamus-specific binding (BP_{ND}) using box and whisker plots.

The University of Manchester
Wolfson Molecular Imaging Centre

Ongoing clinical research studies: psoriasis

- Psoriasis is a chronic inflammatory, immune-mediated skin condition.
- It is associated with multiple co-morbidities and is widely regarded as a systemic inflammatory condition.
- Human (Drake C *et al*. Brain Behav Immun 2011; **25**: 1113-22) and animal (Hannestad J *et al*. Neuroimage 2012; **63**: 232-9) studies have demonstrated that peripheral inflammatory insults can induce brain neuroinflammation.

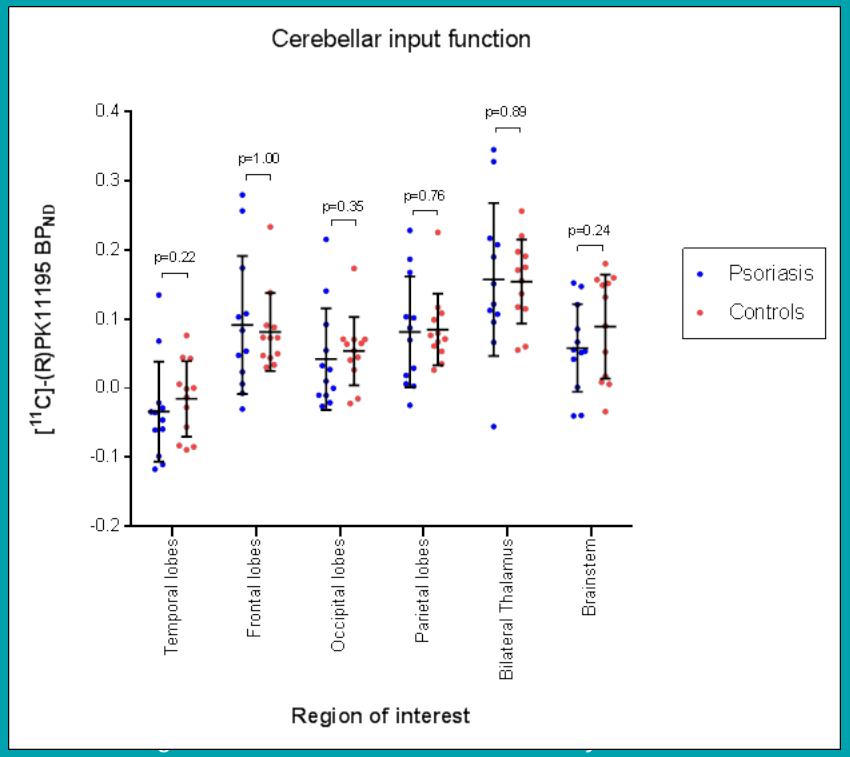

- Case-controlled cohort study (12 psoriasis patients and 12 controls)
- Bars show mean and standard deviation BP_{ND}, *p* values derived from Mann-Whitney U test.
- **No significant difference for either input function (cerebellum, SVCA6).**

Hunter H *et al.* Is psoriasis associated with neuroinflammation? NRM'2014, Egmond aan Zee, 21 - 24 May, 2014.

The University of Manchester
Wolfson Molecular Imaging Centre

MANCHESTER 1824

Ongoing clinical research studies: depression and schizophrenia

- Both major depressive disorder (MDD) and schizophrenia are thought to be associated with neuroinflammation.
- A recent PET study found no evidence for neuroinflammation in mild-to-moderate MDD (Hannestad J *et al*. Brain Behav Immun 2013; **33**: 131-8).
- Two PET studies in schizophrenia have shown evidence for neuroinflammation (Van Berckel BN *et al.* Biol Psychiatry 2008; **64**: 820-2 and Doorduin J *et al.* J Nucl Med 2009; **50**: 1801-7).
- These initial studies might be confounded by mild severity, antidepressant/ antipsychotic medication and low numbers.
- We present an interim analysis of a study investigating neuroinflammation in mostly medication-free, moderate-to-severe MDD and schizophrenia.

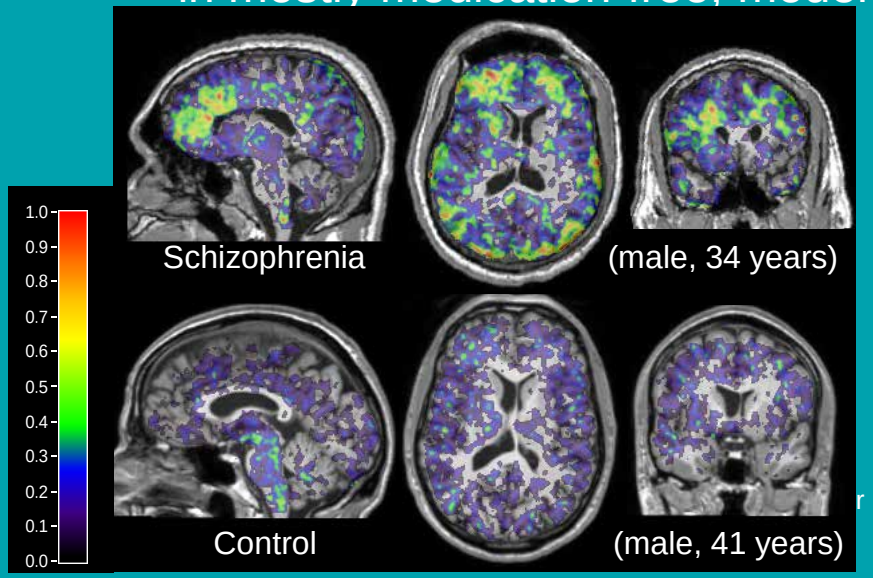

- Grey matter cerebellum input function was used to generate parametric maps of BP_{ND} using the Simplified Reference Tissue Model.

The University of Manchester
Wolfson Molecular Imaging Centre

MANCHESTER 1824

Ongoing clinical research studies: depression and schizophrenia

- 8 patients with a diagnosis of DSM-IV MDD, 8 with schizophrenia and 8 age and gender matched healthy controls.
- All MDD patients were antidepressant-free and 6 of the 8 schizophrenia patients were antipsychotic-free for at least 3 months prior to scanning. All patients had moderate-to-severe symptom severity.

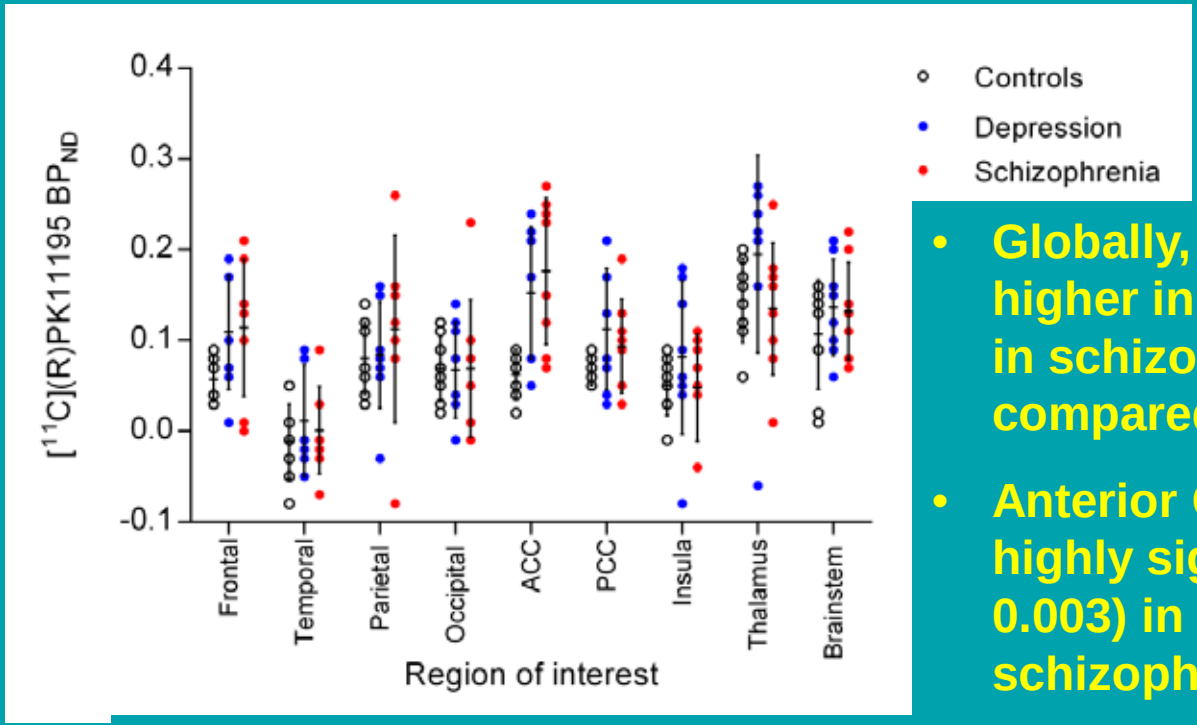

- **Globally, mean BP_{ND} values were higher in depression (0.12 ± 0.06) and in schizophrenia (0.10 ± 0.05) compared to controls (0.07 ± 0.04).**
- **Anterior Cingulate Cortex (ACC): highly significant increases ($p < 0.003$) in both depression and schizophrenia relative to controls.**

Holmes S *et al.* Evidence for neuroinflammation in major depressive disorder and schizophrenia: A PET study using [^{11}C]-(R)-PK11195. BAP Summer Meeting, Cambridge, 20 - 23 July, 2014.

Developments in pre-clinical data analysis

For rodent scans, measurement of plasma input functions is challenging.

Aim: Adaptation of the clinical SVCA to rat brain scans with [^{11}C](*R*)-PK11195.

Six male Wistar rats

Siemens Inveon small animal PET-CT

Stroke model: middle cerebral artery occlusion (MCAO)

1. Core of infarct = activated tissue
2. Contralateral region = normal tissue
3. Cerebellar region = intermediate binding

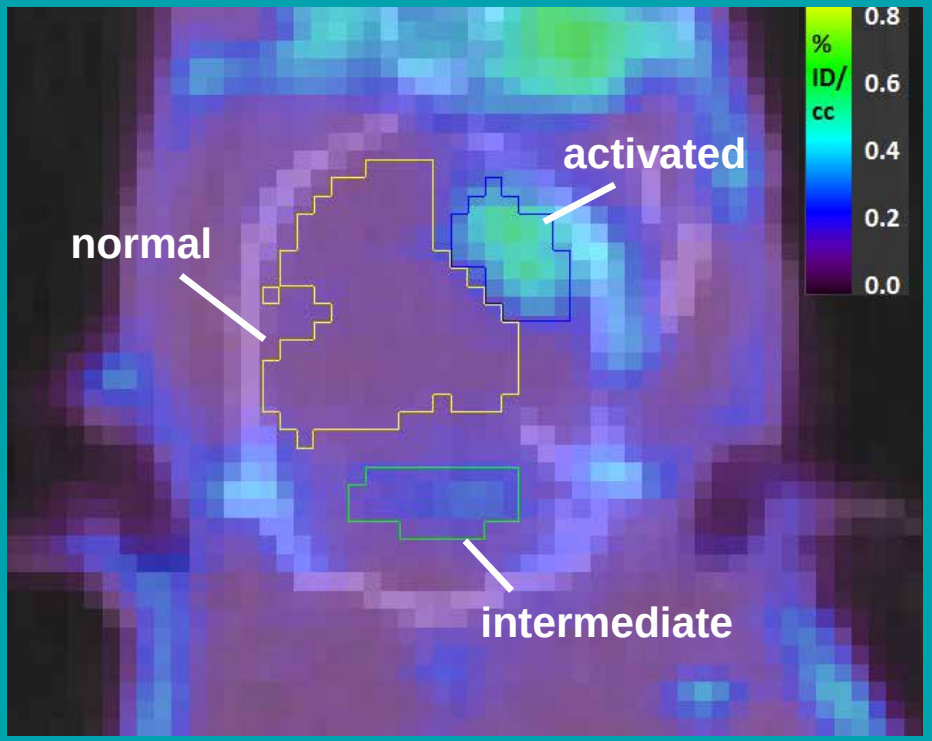

The University of Manchester
Wolfson Molecular Imaging Centre

MANCHESTER 1824

Developments in pre-clinical data analysis

Time-activity curves (TACs) for the three regions identified in the brain of sample animal.

Data normalised, sampled and averaged across animals.

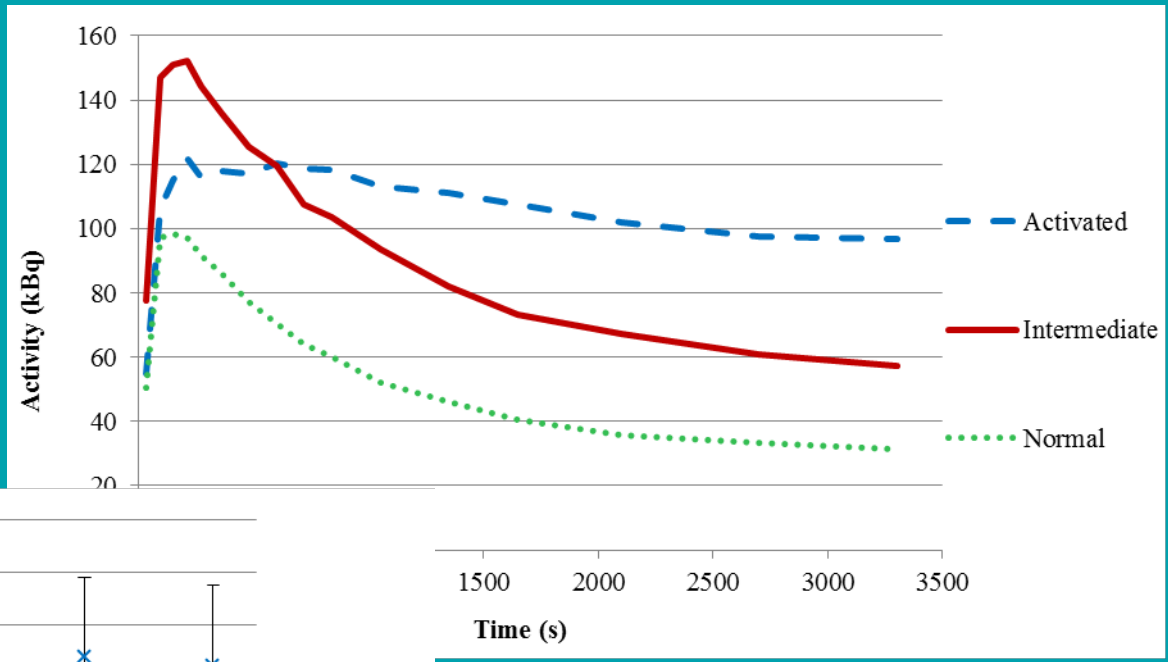

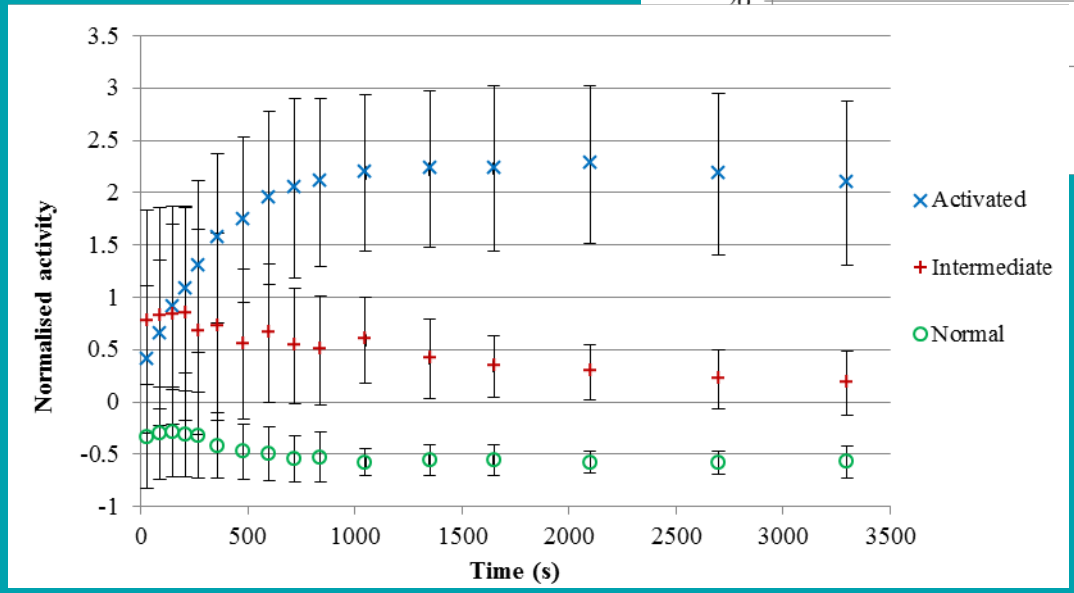

Corresponding normalised TACs forming population database with three classes, averaged across animals, with standard deviations.

Sridharan S *et al.* A data-driven method for automatic extraction of a reference tissue kinetic from [^{11}C]-(R)-PK11195 rodent brain scans. XIII Turku PET Symposium, 24 - 27 May, 2014.

Outlook

Lipopolysaccharide (LPS, bacterial endotoxin)- induced microglial activation to preserve integrity of the blood-brain barrier, doses of 1, 5 and 10 µg

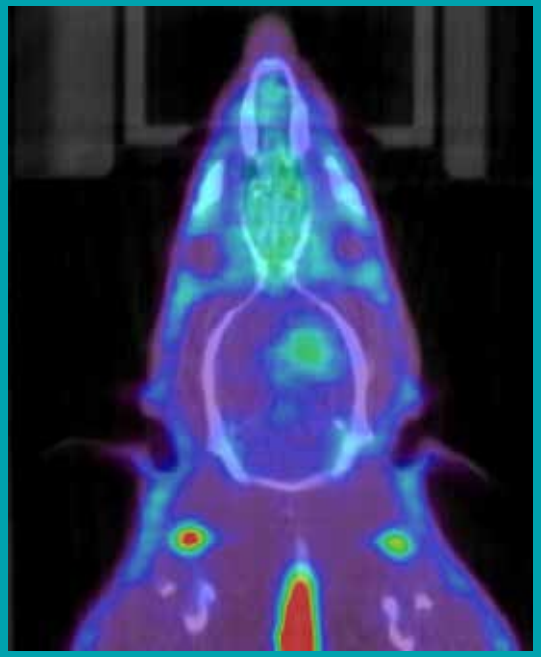

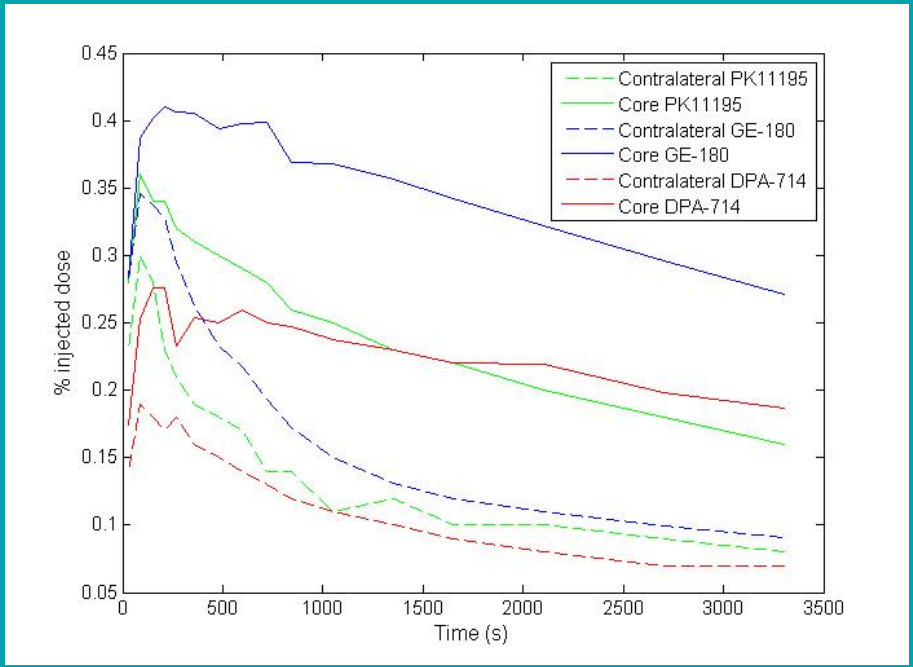

BP_{ND} with SRTM (mean±SD)	10 µg	5 µg	1 µg
[^{11}C](*R*)-PK11195	2.25 (n=1)	3.20 ± 0.30 (n=2)	2.14 ± 0.42 (n=3)
[^{18}F]GE-180	4.04 (n=1)	2.96 ± 0.07 (n=2)	2.49 ± 0.76 (n=6)
[^{18}F]DPA-714	2.53 (n=1)	4.21 ± 0.02 (n=2)	2.95 ± 0.44 (n=5)

The University of Manchester
Wolfson Molecular Imaging Centre

MANCHESTER 1824

Outlook

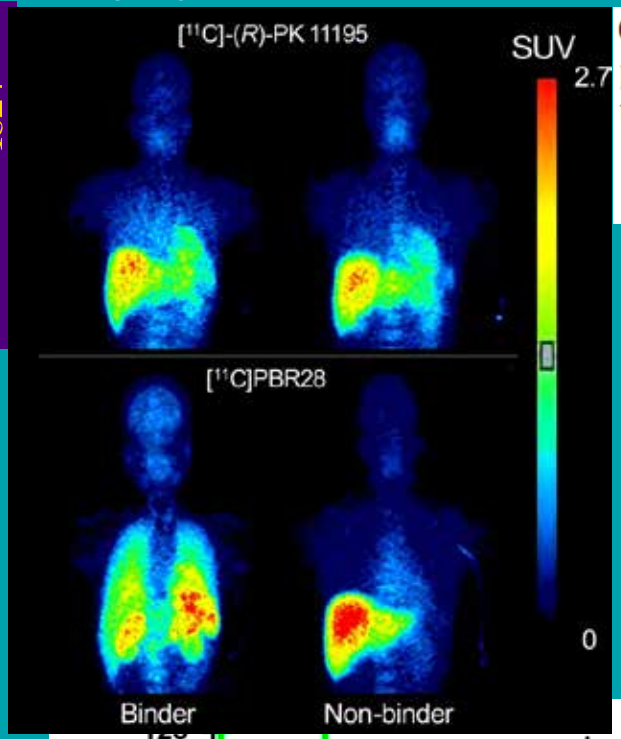

Comparison of [^{11}C]-(*R*)-PK 11195 and [^{11}C]PBR28, two radioligands for translocator protein (18 kDa) in human and monkey: Implications for positron emission tomographic imaging of this inflammation biomarker

William C. Kreisl [a,*], Masahiro Fujita [a], Yota Fujimura [a,c], Nobuyo Kimura [a], Kimberly J. Jenko [a], Pavitra Kannan [a], Jinsoo Hong [a], Cheryl L. Morse [a], Sami S. Zoghbi [a], Robert L. Gladding [a], Steven Jacobson [b], Unsong Oh [b], Victor W. Pike [a], Robert B. Innis [a,*]

NeuroImage 49 (2010) 2924–2932

An 18-kDa Translocator Protein (TSPO) polymorphism explains differences in binding affinity of the PET radioligand PBR28

David R Owen[1,2,6], Astrid J Yeo[3,6], Roger N Gunn[2,4,5], Kijoung Song[3], Graham Wadsworth[2], Andrew Lewis[1], Chris Rhodes[1], David J Pulford[3], Idriss Bennacef[2], Christine A Parker[2,4], Pamela L StJean[3], Lon R Cardon[3], Vincent E Mooser[3], Paul M Matthews[2,4], Eugenii A Rabiner[2,4] and Justin P Rubio[3]

Journal of Cerebral Blood Flow & Metabolism (2012) 32, 1–5

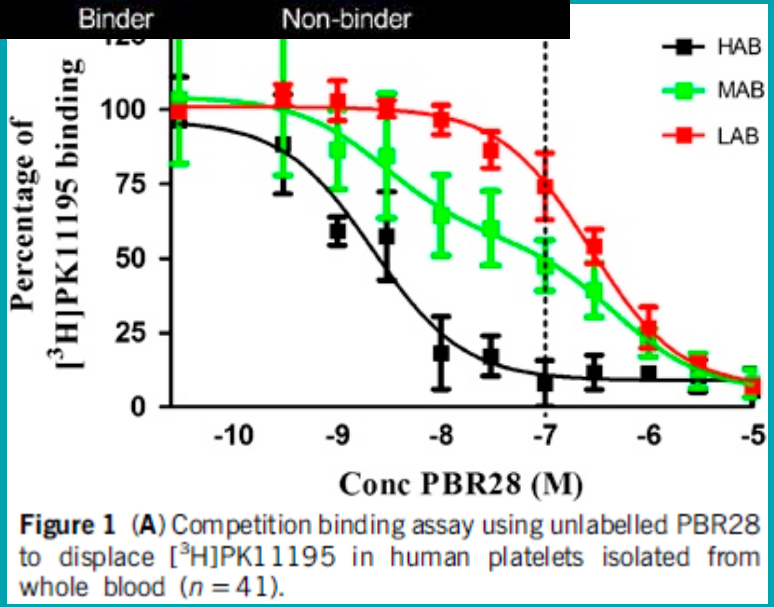

Figure 1 (**A**) Competition binding assay using unlabelled PBR28 to displace [^{3}H]PK11195 in human platelets isolated from whole blood ($n = 41$).

Table 1 Distribution of rs6971 genotypes against ligand binding classification

TSPO genotype		*Binding phenotype (subject, n)*		
DNA (polymorphism rs6971)	*Protein (position 147)*	*HAB*	*MAB*	*LAB*
C/C	Ala/Ala	27		
C/T	Ala/Thr		12	
T/T	Thr/Thr			2

Ala = alanine, Thr = threonine, HAB = high affinity binder, MAB = mixed affinity binder, LAB = low affinity binder.
Genotypes correspond to carriage of the 147 amino acid as follows: CC = Ala147/Ala147; CT = Ala147/Thr147; TT = Thr147/Thr147.

The University of Manchester
Wolfson Molecular Imaging Centre

MANCHESTER 1824

Outlook

Determination of [^{11}C]PBR28 binding potential *in vivo*: a first human TSPO blocking study

Journal of Cerebral Blood Flow & Metabolism (2014) 34, 989–994

David R Owen[1], Qi Guo[1,2,3], Nicola J Kalk[1,3], Alessandro Colasanti[1,3], Dimitra Kalogiannopoulou[4], Rahul Dimber[3], Yvonne L Lewis[3], Vincenzo Libri[4], Julien Barletta[3], Joaquim Ramada-Magalhaes[3], Aruloly Kamalakaran[3], David J Nutt[1], Jan Passchier[3], Paul M Matthews[1,5], Roger N Gunn[1,3] and Eugenii A Rabiner[2,3]

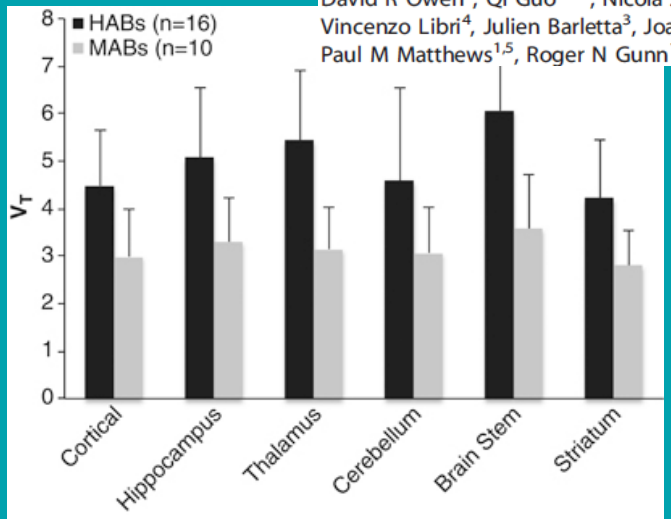

Figure 1. Effect of genotype on ^{11}C-PBR28 total volume of distribution in high-affinity binders (HABs) ($n = 16$) and mixed affinity binders (MABs) ($n = 10$).

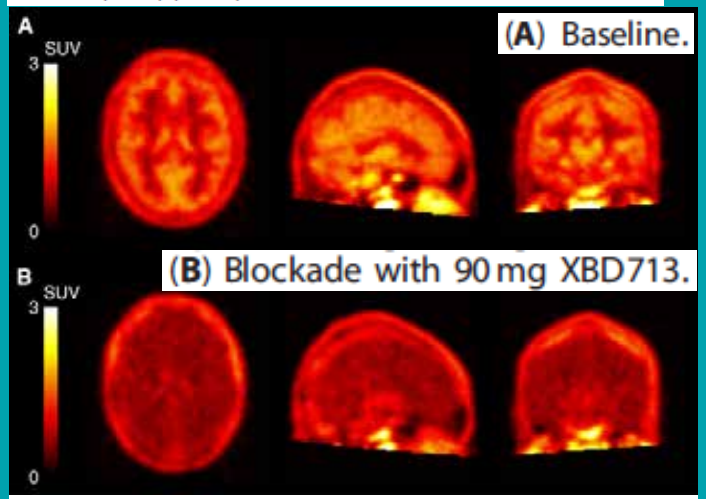

Figure 2. Integral images (0 to 90 minutes) of [^{11}C]PBR28 in a high-affinity binders (subject 11) before and after blockade.

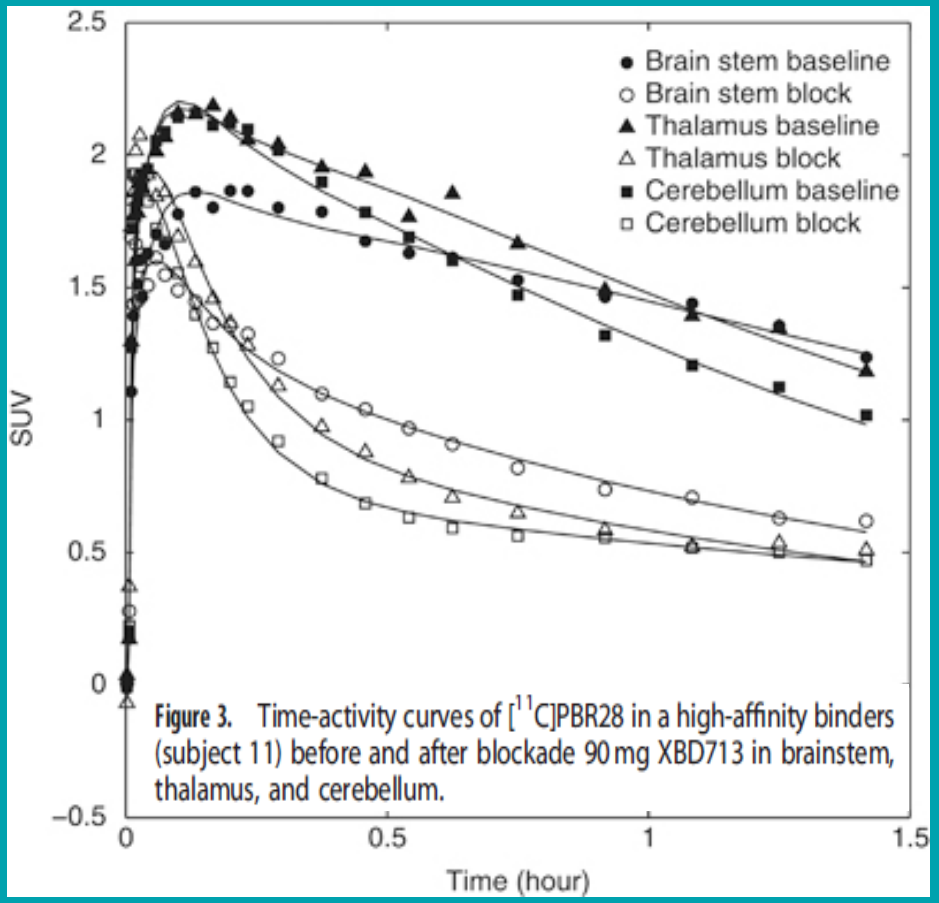

Figure 3. Time-activity curves of [^{11}C]PBR28 in a high-affinity binders (subject 11) before and after blockade 90 mg XBD713 in brainstem, thalamus, and cerebellum.

Reference region?

The University of Manchester
Wolfson Molecular Imaging Centre

MANCHESTER 1824

Acknowledgements

PhD students and Clinical Fellows

- David Coope, Matthew Jones
- Salman Karim, Zangjie Su
- Kamran Abid, Hamish Hunter
- Glenn Holland, Sophie Holmes
- Sujata Sridharan

Clinical PIs

- Pippa Tyrrell, Alistair Burns
- Karl Herholz, Alan Jackson
- Alex Gerhard, Peter Talbot
- Elise Kleyn, Chris Griffiths
- Adrian Parry-Jones

Colleagues and Collaborators

- Hervé Boutin
- Federico Turkheimer (London)
- Ronald Boellaard (Amsterdam)
- Chris Buckley (GE Healthcare)

Study volunteers and staff at the Wolfson Molecular Imaging Centre.